Entanglement Assembly of Graphite Worms: A Direct Strategy to Achieve Highly Crystalline Graphene Foam for Superior Electromagnetic Interference Shielding

Wenyu Wu[a,*], Man Qi[a], Ling Wang[a], Nan Gao[a], Pengtao Yan[b,*], Wenwen Liu[a], Jianzhi Sun[a], Zhigang Wang[a], Longlong Geng[a], Ruijun Zhang[c,*]

[a] Shandong Provincial Key Laboratory of Monocrystalline Silicon Semiconductor Materials and Technology, College of Chemistry and Chemical Engineering, Dezhou University, Dezhou 253023, China.

[b] School of Physics and Electronic Engineering, Xingtai University, Xingtai 054001, China.

[c] State Key Laboratory of Metastable Materials Science and Technology, Yanshan University, Qinhuangdao 066004, China.

[*] Corresponding author.

E-mail address: wenyuwuky@163.com (W. Wu), 201710995@xttc.edu.cn (P. Yan), zhangrj@ysu.edu.cn (R. Zhang).

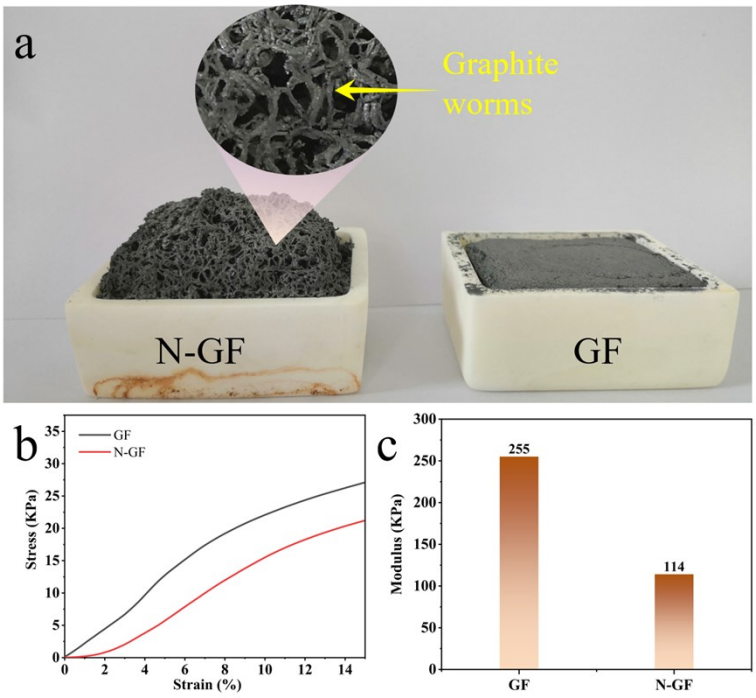

Fig. S1. (a) Macroscopic photographs of GF and N-GF. (b) Compressive stress-strain curves of GF and N-GF. (c) Comparison of the compressive modulus at 5% strain for GF and N-GF.

To validate the critical role of the confined expansion-induced entanglement mechanism, a control experiment was conducted by performing the expansion reaction in an open container (denoted as N-GF) under otherwise identical conditions. As shown in Fig. S1a, N-GF exhibited a loose and discontinuous structure with poorly entangled graphite worms and visible macroscopic gaps. In contrast, GF formed a coherent, self-supporting foam. Compression tests (Fig. S1b and c) revealed that the compressive modulus of N-GF at 5% strain was only 114 kPa, less than half that of GF (255 kPa). These results quantitatively confirm that spatial confinement-induced entanglement is essential for the mechanical integrity and network continuity of the resulting graphene foam.

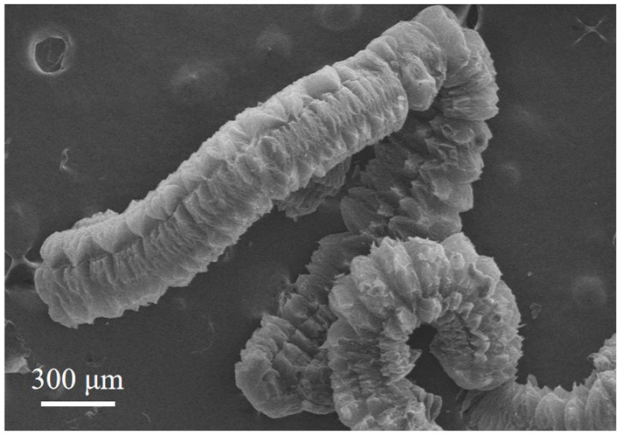

Fig. S2. SEM image of an isolated graphite worm obtained from a control experiment conducted in an open container. The preparation conditions were identical to those used for GF, except that the expansion reaction was carried out in an open environment to prevent entanglement and allow the isolation of individual worms.

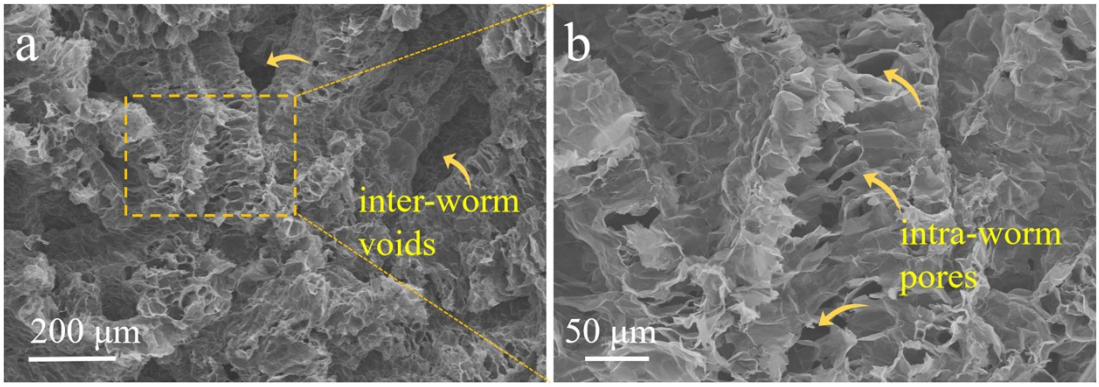

Fig. S3. Representative SEM images of GF illustrating its multi-scale porous architecture.(a) Low-magnification image showing the continuous network of entangled graphite worms and the larger inter-worm voids (typical size: ~50-200 μm) that dominate the macroscopic foam structure. (b) Higher-magnification image revealing the finer intra-worm pores (typical size: ~5-20 μm) within an individual graphite worm. This hierarchical porosity, spanning tens to hundreds of micrometers, is crucial for efficient electromagnetic wave dissipation.

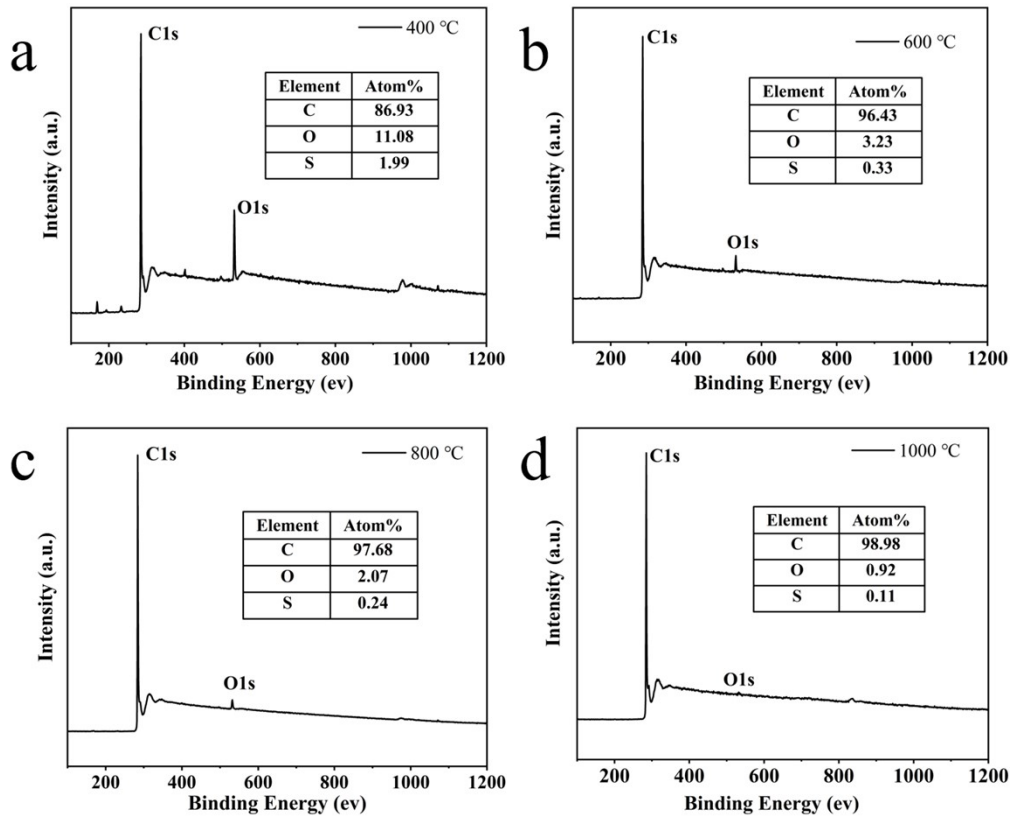

Fig. S4. XPS survey spectrum of GF-2.5 annealed at different temperatures. (a) 400 ℃, (b) 600 ℃, (c) 800 ℃ and (d) 1000 ℃.

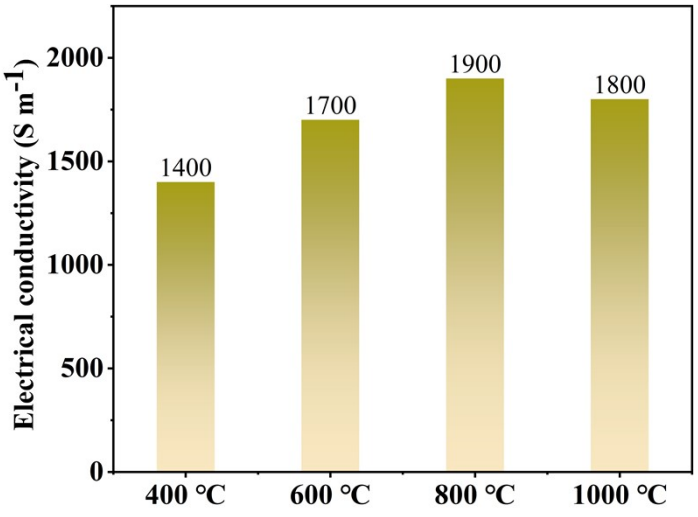

Fig. S5. Electrical conductivity of GF-2.5 annealed at different temperatures.

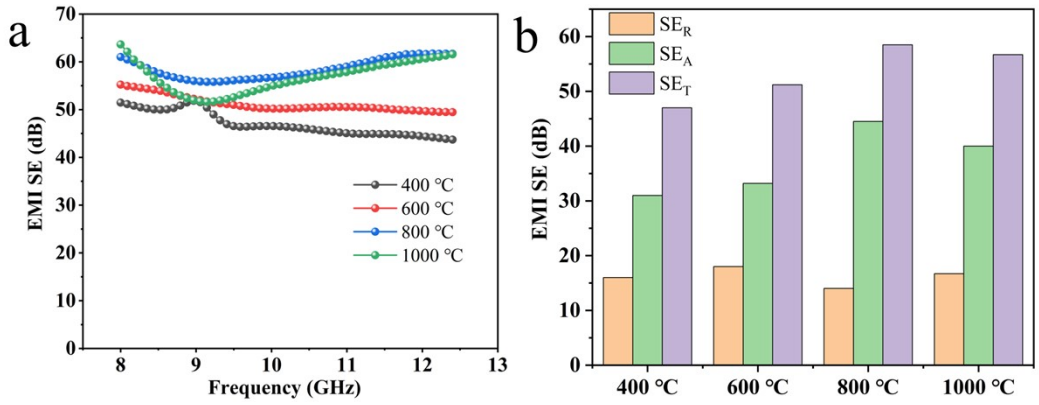

Fig. S6. (a) EMI SE across the X-band for GF-2.5 samples annealed at different temperatures. (b) The average SE_T, SE_A and SE_R values for GF-2.5 samples annealed at different temperatures.

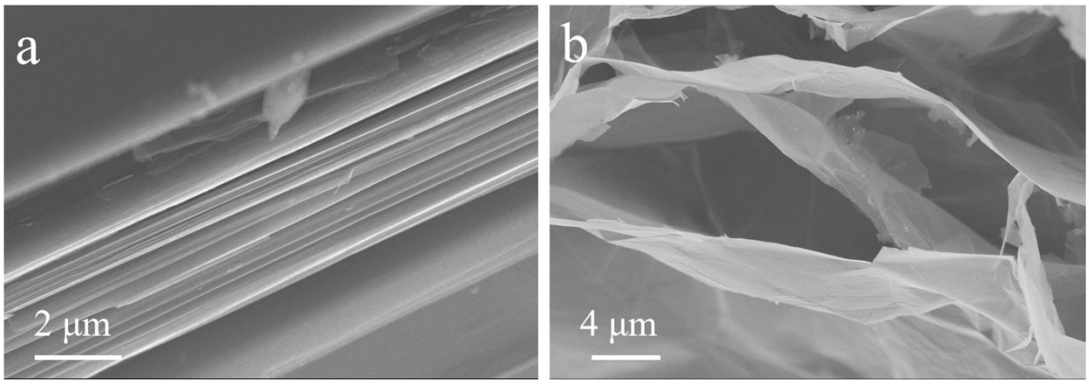

Fig. S7. Cross-sectional SEM images showing the morphological evolution from NG to GF-2.5. (a) NG exhibiting a highly ordered and densely stacked lamellar structure with negligible interlayer spacing. (b) GF-2.5 foam after confined expansion and thermal treatment, displaying a dramatically expanded architecture with interlayer distances on the order of several micrometers.

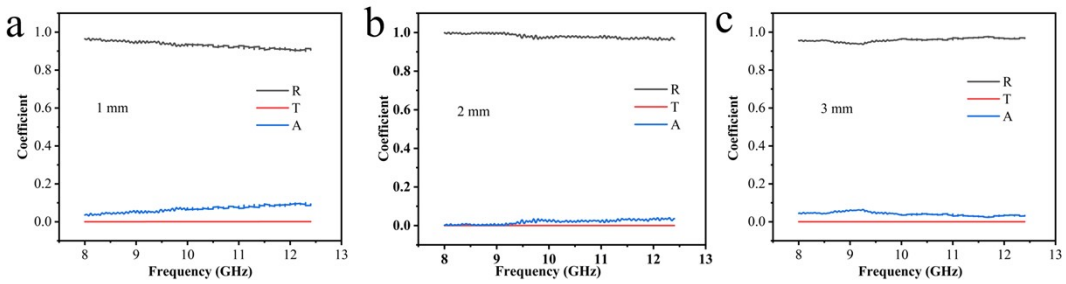

Fig. S8. A, R and T values of GF-2.5 samples at different thickness: (a) 1 mm, (b) 2 mm, (c) 3 mm. A is absorption coefficient, R is reflection coefficient, and T is transmission coefficient.

Table S1. Elemental composition of GF-2.5 determined by EDS quantitative analysis.

Element	Atomic Percentage (at%)
C	97.67
O	1.94
S	0.38

Table S2. Contrast of EMI shielding performance of the carbon-based shielding materials.

Sample	Thickness (mm)	Density (mg cm^{-3})	Frequency (GHz)	EMI SE (dB)	SSE/t (dB cm^2 g^{-1})	Ref.
CNT/CS foam	2.5	17.6	8.2~12.4	37.6	8545.5	[46]
CNT@G/Cs	2.5	1050	8.2~12.4	45.3	172.4	[47]
ANF/GN aerogel	2	40	8.2~12.4	31.55	3878.8	[48]
RGO aerogel	2.5	5.56	8.2~12.4	20.4	14676.3	[49]
C-ZIF67/GNP film	0.1	1180	8.2~12.4	50.5	4280	[50]
PEN/5G3C foam	1.6	200	8.2~12.4	25.8	806.3	[51]
Graphene aerogel	3	70	8.2~12.4	37	1761.9	[52]
CNWs/G composite	1.6	97.1	8.2~12.4	36	2319.6	[53]
GF/Fe_3O_4/PDMS composite	0.3	650	8.2~12.4	71	3641	[54]
MWCNT/WPU composite	1	39	8.2~12.4	21.1	5410	[55]
Graphene foam	1	17.2	8.2~12.4	33.2	19302.3	This work